NOVEL PROCESS USING OXYGEN AND AIR BUBBLING IN CHEMICAL BATH DEPOSITION METHOD FOR VERTICALLY WELL ALIGNED ARRAYS OF ZnO NANORODS

A. F. ABDULRAHMAN[a*], S. M. AHMED[b], N. M. AHMED[c], M. A. ALMESSIERE[d]

[a]*Physics Department, Faculty of Science, University of Zakho, Zakho, Kurdistan Region, Iraq*

[b]*Physics Department, Faculty of Science, University of Duhok, Duhok, Kurdistan Region, Iraq*

[c]*Nano-Optoelectronic Research & Technology Laboratory, School of Physics, Universiti Sains Malaysia, Penang, Malaysia*

[d]*Physics Department, Collage of Science, University of Dammam, Dammam, Kingdom of Saudi Arabia*

Vertically well-aligned ZnO nanorods arrays have been synthesized on ZnO seed layer coated glass substrates at low temperature using modified low-cost chemical bath deposition (CBD) method. The investigation of the influence of no air bubbles, air bubbles and oxygen bubbles inside the CBD reactor on the structural characteristics, morphological (diameter, length, aligned, distribution and homogeneously), elements chemical composition and optical properties of ZnO nanorods have been studied. This new modification of chemical bath deposition method shows the improved results over traditional chemical bath deposition method. The important results of this novel process are the good morphological, structural characteristic and optical properties of ZnO nanorods. These results obtained in just of 3.5 h growing time in the CBD reactor. On this modified CBD the growth time rate decreases about 1.5 h compared with the previous works.

(Received August 3, 2016; Accepted October 11, 2016)

Keywads: Novel Process, Semiconductors, Oxygen & Air Bubbling, Optical Properties, Crystal Structure, X-ray Diffraction, ZnO Nanorods.

1. Introduction

Zinc oxide (ZnO) is an essential metal oxide member of group II-VI semiconductor materials. It has attracted great interest because of its direct wide band gap (3.37 eV) and high exciton binding energy (60 meV, 2.4 times the thermal energy at room temperature (25 meV)) [1]. These properties make ZnO a more promising material in excitonic emissions and lasing applications above room temperature compared with other materials. In addition to its chemicals and thermal properties, ZnO also has photo conducting and piezoelectric properties. Therefore, it has possibility for a large domain of implementations, such as for light emitting diode (LED), biomedical uses, UV optical devices, solar cells and gas sensing applications [2-6].

ZnO can also be synthesized in various nanostructure forms, such as nanowires, nanorods, nanoflowers, nanoparticles, and other [7-10]. These nanostructures exhibit two excellent properties, namely, high surface area to volume ratio and quantum effects which are not observed in its bulk nature. These unique nanostructure properties renewed the wide range of applications of ZnO nanomaterials. One dimensional (1D) ZnO nanorods have been synthesized using various preparation procedures that can be classified as low (<100^{o}C) and high (>100^{o}C) temperature [11, 12]. High temperature synthesis includes metal organic chemical vapor deposition (MOCVD) [13], electrochemical deposition [14], pulsed laser deposition [15], spray pyrolysis [16], epitaxial

* Corresponding author: ahmadamedi@yahoo.com

electrodeposition [17], and radio frequency magnetron sputtering [18] chemical vapor deposition and molecular beam epitaxial (MBE) [19]. Low temperature synthesis is derived from chemical solution methods, which can be divided into solvothermal, hydrothermal [20] and low cost chemical bath deposition (CBD) method [21]. Recent studies have synthesized nanomaterials by chemical solution techniques because of their low synthesis temperature requirement, low cost, and high production scale [11, 12].

However, CBD syntheses have problematic for three reasons [22, 23]. First, it is difficult to maintain the homogeneity of the concentration of the solution in the bath during growth process. The homogeneity of the solution (chemicals) depends on the densities of precursors. Second, it is difficult to direct supply thermal energy to the substrate because the entire bath is heated, which can cause unwanted homogeneous reactions to occur in the solution, hindering growth on the substrate. Third, even the heating of the CBD reactor in oven and there is a time for temperature equilibrium for the solution, but still we believe there is a temperature gradient in CBD reactor because there is no stirring way inside the oven.

In this paper, to address these problems, a modified CBD (M-CBD) process by introducing the stirring way to the solution of the CBD reactor inside the oven. Continuously delivers a constant concentration of solution to the substrate, reduces the likelihood of homogeneous reaction and provide the oxygen during the CBD reaction by bubbles the air and oxygen inside the solution of the CBD reactor. A modified CBD process and the investigation of the effects of the synthesis with and without air and oxygen bubbles on the growth of ZnO nanorods on seeded glass substrates have been studied. This new modified CBD process produced vertically aligned grown ZnO nanorods with a high growth rate and good structural XRD properties with good agreement of optical energy band gap and optical properties. The results indicates that the this modified CBD process can be apply for all different parameters that can be change to get the vertically aligned of ZnO nanorods such concentration, growth time, bath temperature, annealing and pH effect.

2. Methodology

2.1 Sample Preparation

All used chemical substances in this paper are of analytical grade from Sigma-Aldrich Company, and utilized as beginning materials without further refinement. In this work, ZnO seed layer coated glass has been used as a substrate for growing ZnO nanorods. This method has been completed in two steps. In the first step, the glass substrates have been cleaned in an ultrasonic bath by using ethanol, acetone and deionized water for 15 min respectively and dried with nitrogen gas. In the second step, a radio frequency (RF) magnetron sputtering was utilized using target (99.999% purity of ZnO) was deposited ZnO seed layer on the cleaned glass substrates. The 100 nm thick ZnO seed layer was deposited on the glass substrates with 5.5 $*10^{-3}$ mbar argon gas pressure inside RF chamber and 150 Watt RF power sputtering for 15 min. After that the prepared ZnO seed layer annealed inside tubular furnace at 400^{o}C for 2 h under atmosphere to stress relief the coated layer.

2.2 Growth Process

For vertical well-aligned ZnO nanorods (ZNR), a low-cost modified CBD method at low temperature has been used. The zinc nitrate hexahydrate (Zn $(NO_3)_2.6H_2O$) and hexamethylenetetramine (HMTA) ($C_6H_{12}N_4$) were used as precursors, and deionized water was employed as a solvent. The appropriate amount of HMTA ($C_6H_{12}N_4$) equal molar concentration of zinc nitrate hexahydrate (Zn $(NO_3)_2.6H_2O$) were separately dissolved in deionized water at 80 ^{o}C and mixed together under magnetic stirrer. The prepared ZnO seed layer was inserted vertically inside a beaker including a mixture of the two solutions. To obtain the effect of the no air bubbles, air bubbles and oxygen gas bubbles inside the CBD process, three CBD reactors (for each case) were placed inside an oven at 95^{o}C for 3.5 h as shown in figure 1. At the end of growth process the three samples were rinsed by deionized water to remove the remaining salt, and then it was dried by nitrogen gas.

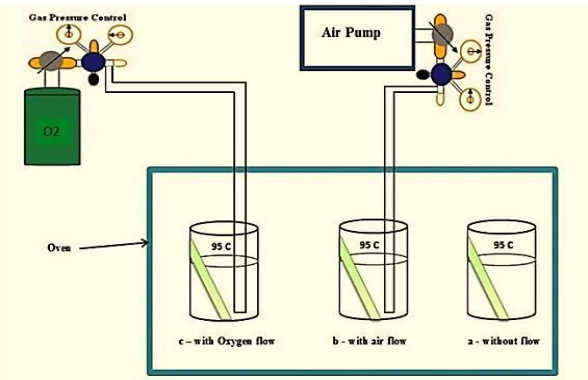

Fig. 1. Schematic diagram (novel process) of modified CBD System

2.3 Characterization Techniques

The surface morphology (Length, diameter, homogeneity, density and distribution of ZnO nanorods), energy dispersive X-ray spectroscopy (EDX) analysis to provide (quantitative and qualitative) analyses of elemental composition of all samples, crystal structure (stress, strain and quality of the epitaxial growth of ZnO nanorods on glass substrates) and energy band gap of the ZnO thin films were obtained from the absorption spectrum are characterized by Field Emission Scanning Electron Microscope (FESEM) (FESEM model is: FEI Nova a nano SEM 450 Netherlands and Leo-Supra 50 VP, Carl Zeiss, Germany), high resolution XRD (HR-XRD) system (X-Pert Pro MRD model with CuKα (λ = 0.154050 nm) radiation and scanning range of 2θ set between 20˚ and 80˚) and a double beam UV visible (UV-4100) spectrometer with a wave length range 300 nm to 1000 nm, respectively.

3. Result and Discussion

3.1 Structure Characteristics:

The X-Ray diffraction patterns of ZnO nanorods grown on glass substrate when there is no air bubbles, air bubbles and oxygen bubbles are displayed in figure 2. Figure 2 (a) shows the diffraction pattern of ZnO nanorods grown on glass substrate with no air bubbles, from the figure one can notice that ZnO nanorods grown in different preferred orientations which they are (100), (002) and (101) and this is proved that the two phases of ZnO grown in this way which they are hexagonal quartzite phase and wurtzite phase [24]. These two phases are characteristics of the pure ZnO. No foreigner diffraction peaks are arising from any impurity in the pattern and this is confirmed that the grown process is pure ZnO. The lattice constants *a* and *c* of the ZnO wurtzite structure can be obtained using Bragg's law, as it's shown in table 1, [25, 26]:

$$a = \sqrt{\frac{1}{3}}\frac{\lambda}{sin\theta} \tag{1}$$

$$c = \frac{\lambda}{sin\theta} \tag{2}$$

Where θ is the angle of the diffraction peak and λ = 0.15405 nm is the wavelength of the X-ray source. The strain (ε_c) of the ZnO nanorod grown on the glass substrate along c-axis can be found by using the following equation [27-29]:

$$\varepsilon_c = \frac{c - c_o}{c_o} * 100\% \tag{3}$$

Where is c_o demonstrating the standard lattice constant for unstrained ZnO which is equal to 5.2098 Å. A negative value is concerned to the compressive strain and indicates a lattice contraction, while a positive value of strain is concerned to the tensile strain and indicates an expansion in lattice constant. The lattice parameters were summarized and listed in Table 1.The results indicate that the CBD method is a fast and cheap route for the fabrication of single phase ZnO nanorods at relatively low temperature.

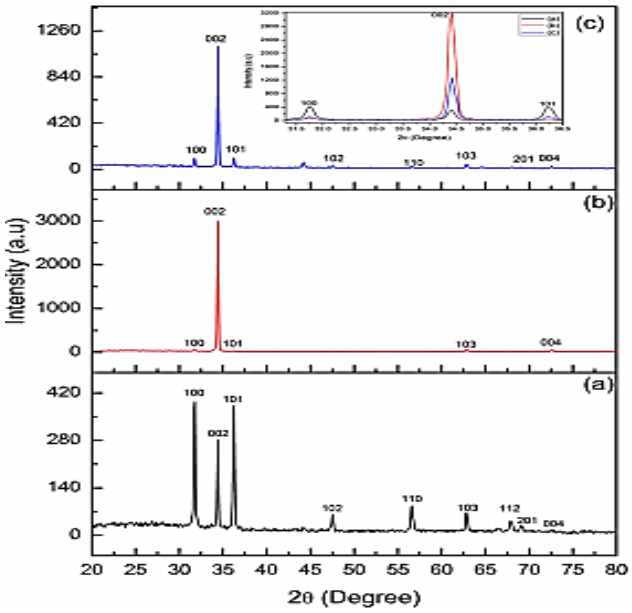

Fig. 2. .X-Ray diffraction patterns of ZnO nanorods
(a) No Air Bubbles, (b) Air Bubbles, (c) Oxygen Bubbles

The one most often utilized approaches in calculating the average crystal size of the X-ray data is the usage of the Debye Scherer formula [30]:

$$D = \frac{K\lambda}{\beta cos\theta} \tag{4}$$

Where, λ is the wavelength of the X-ray used (1.54056 Å), k is a constant which is taken to be 0.9, θ is the Braggs diffraction angle and the β is the full width at half maximum of the peak. The dislocation density (δ), which represents the amount of defects in the crystal, is calculated by [31]:

$$\delta = \frac{1}{D^2} \tag{5}$$

Where D is the average crystal size. The plane spacing of wurtzite hexagonal structure of zinc oxide (ZnO) can be calculated according to Bragg's law Equation 1 and 2 which is related to miller indices by following equation [25]:

$$2dsin\theta = n\lambda \tag{6}$$

Where λ is X-ray wavelength, n is the order of diffraction that usually is 1 and *d* in the plane spacing. The structural properties of the ZnO nanorods where is no air bubbles are shown in Table 1.

Table 1 lattice parameters and structure properties of the ZnO nanorods where is no air bubbles

Sample	plan	a (Å)	c (Å)	d (Å)	FWHM(β)^o	2θ^o	D (nm)	ε_c%	Intensity	δ (nm)$^{-2}$
No Air Bubbles	100	3.251759	5.63221	2.81611	0.5904	31.7493	13.9893	+8.10805	398	0.0051098
	002	3.005800	5.206199	2.603099	0.1481	34.4250	56.15641	- 0.06911	283	0.000317
	101	2.857497	4.94933	2.47467	0.7872	36.2721	10.6194	- 4.99961	387	0.008874

The crystal structure of the as-grown ZnO nanorods prepared in CBD process with an air bubbles are investigated by XRD pattern as shown in figure 2 (b). It is observed that the as-grown ZnO nanorods are hexagonal structure, the remarkably sharp peak at 34.3928 is assigned to be the [002] peak of hexagonal maximum (FWHM) is 0.7872, the strong and narrow indicates that the as-grown sample have good crystallinity and preferentially oriented along the c-axis as well as perpendicular to the substrate surface which is well in agreement with the FESEM image. From the analysis of the growth mechanism of vertically well-aligned ZnO nanorods, one can notice that the air bubbles play a very important role. The lattice parameters of hexagonal and structure properties of the ZnO nanorods are shown in table 2.

Table 2 lattice parameters and structure properties of the ZnO nanorods where is air bubbles

Sample	plan	a (Å)	c (Å)	d (Å)	FWHM(β)^o	2θ^o	D (nm)	ε_c%	Intensity	δ (nm)$^{-2}$
Air Bubbles	002	3.00852928	5.210926	2.605463	0.7872	34.3928	10.56406	+ 0.021613	3206	0.008961

Fig. 2 (c) shows the X-ray diffraction pattern of the ZnO nanorods prepared using oxygen bubbles inside the beaker during the CBD growth. All the diffraction beaks in the pattern have been indexed as the hexagonal phase of ZnO with space group P63mc. The lattice parameters have been calculated and are found to be a= 3.00852928 Å and c= 5.210926 Å and are in good agreement with the reported standard values (JCPDS cards No. 01-080-0075). Besides, no diffraction peaks from other impurities have been observed. The lattice parameters of hexagonal and structure properties of the ZnO nanorods are shown in table 3.

Table 3 lattice parameters and structure properties of the ZnO nanorods where is Oxygen bubbles

Sample	plan	a (Å)	c (Å)	d (Å)	FWHM(β)^o	2θ^o	D (nm)	ε_c%	Intensity	δ (nm)$^{-2}$
Oxygen Bubbles	002	3.00852928	5.210926	2.605463	0.7872	34.3928	10.56406	+ 0.021613	1273	0.008961

The crystallinity of ZnO nanorods and aligned nanorods may be important parameters because the electron transfer is also determined by grain size [32]. One effective method to modify the surface condition and crystallinity of ZnO nanorods is air and oxygen bubbles during the CBD growths, which change the diameter and aligned the nanorods. Air and oxygen bubbles also improve the crystallinity of ZnO by decreasing the oxygen vacancy concentration and deep level defects or surface defect recombination.

3.2 Morphology Characteristics

The surface morphology, diameter, distribution and homogeneity of ZnO nanorods fabricated by new low-cost modified CBD method for the three cases are displayed in figure 3. Figure 3 (a) shows the ZnO nanorods grown with no air bubbles inside the CBD growth process. It was observed that the nucleation of ZnO nanorods occurred on the surface of the seed layer and the distribution of the nanorods was randomly oriented and ZnO nanorods has no vertically well

aligned on the substrate with a diameter of (78.805 nm). One believed that is may be coming from the fact there is no homogeneity in chemicals of the solution.

Also figure 3 (b) reveal the ZnO nanorods grown under an air bubbles inside the CBD growth process with flow rate of 5 lit. /min and air pressure 0.7 bar, it can be seen that the ZnO nanorods have good distribution with good uniform orientation and have hexagonal ZnO nanorods with a diameter of (140.725nm) and has vertically well-aligned of ZnO nanorods grown on the seeded coated glass substrate. This is may be due to the air bubbles agitate the solution inside the CBD reactor increasing the homogeneity of the solution in the CBD process. The heavy precursors are precipitated at the bottom of the beaker and this is the problem when the air bubbles process not used, in the first case of no air bubbles there is no uniform distribution of the ZnO nanorods over the sample, and the second case when providing the bubbles rate of air for the CBD which is help the ZnO nanorods in grown more aligned and getting the exact hexagonal orientation and uniform over the sample.

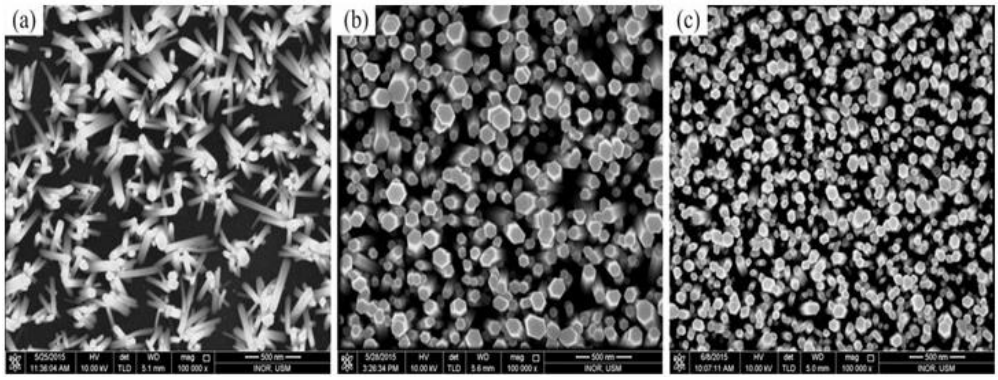

Fig. 3. The FESEM images of ZnO nanorods prepared by modified CBD
(a). No Air Bubbles, (b). Air Bubbles, (c) Oxygen Bubbles

In Addition figure 3 (c) shows the vertically aligned ZnO nanorods along the c-axis with a high distribution density of rods over the entire substrate for oxygen flow rate 5 lit./min and 0.7 bar oxygen pressure. It can be seen that the orientation of ZnO nanorods is uniform and have a hexagonal shape with a diameter of (98.99 nm). This is due to the same previous reasons of air bubbles.

From figures 3(b) and 3(c) one can notice that the ZnO nanorods prepared by introducing oxygen bubbles are denser and less diameter than ZnO nanorods produced by introducing air bubbles.

The Cross-Section, length and aligned of ZnO nanorods synthesized by novel modified low-cost chemical bath deposition (CBD) method for the three cases shown in figure 4. Figure 4 (a) shows the cross-section, length and aligned of ZnO nanorods when there is no air bubbles inside the chemical bath deposition process. It was observed that the ZnO nanorods are not well vertically aligned it means it have different height, direction and the bottom of the nanorods wider than the top of its. The length of ZnO nanorods is about (725 nm). The reason of non-aligned nanorods is as explained in previous section for the same case.

The cross-section, length and aligned of ZnO nanorods grown under an air bubbles inside the CBD growth process with flow rate 5 lit. /min with air pressure is 0.7 bar is shown in figure 4 (b). It can be seen that the ZnO nanorods have vertically well-aligned with good uniform orientation, uniform height and have hexagonal ZnO nanorods with a length of (1.093 μm). This is may be due to the same previous reasons (above reasons). In addition figure 4 (c) shows the vertically well-aligned with dens distribution, cross-section and length of ZnO nanorods where oxygen bubbles inside beaker during chemical bath process. It can clearly see that the ZnO nanorods have a good distribution compare to the no air bubbles and has hexagonal shape and its length is about (680 nm) this is due also to the same reasons described in the above section.

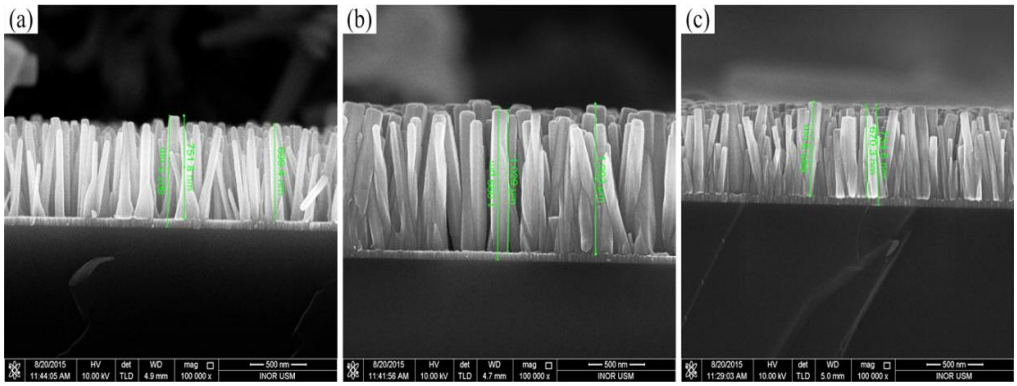

Fig. 4. The Cross-Section of ZnO nanorods prepared by modified CBD
(a). No Air Bubbles, (b). Air Bubbles, (c) Oxygen Bubbles

3.3 Energy Dispersive X-Ray Analysis (EDX):

The elemental chemical composition (quantitative and qualitative) of the as-grown ZnO nanorods fabricated by modified chemical bath deposition process on glass substrates at 95^{o}C for 3.5 h are examined by EDX as shown in figure 5. Figure 5 (a) reveal the typical quantitative EDX analysis for as grown ZnO nanorods (prepared with no air bubbles), from the figure one can notice that the elementary chemical compositions for the grown nanorods are zinc and oxygen only. The molecular ratio of Zn:O of the grown nanorods, calculated from EDX and quantitative analysis data, is close to that of 1:1. The EDX spectrum confirmed that the grown nanorods are pure ZnO. Also figures 5 (b & c) shows the quantitative EDX analysis for the nanorods prepared with an air bubbles and oxygen gas bubbles in CBD reactor. The EDX spectrum confirmed also that the grown nanorods are pure ZnO.

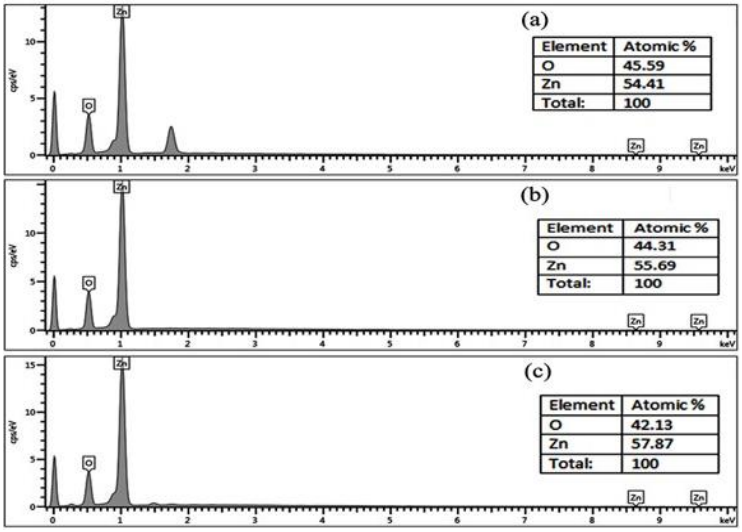

Fig. 5. Typical EDX analysis with it quantity that the grown nanorods prepared by modified CBD
(a). No Air Bubbles, (b) Air Bubbles, (c) Oxygen Bubbles

3.4 Optical Properties of the ZnO nanorods:

The energy band gap of ZnO thin films was measured from the absorption spectra by using a double beam UV, visible (UV-4100) spectrometer with a wavelength range from 300 nm to 1000 nm. Figure 6 shows the optical absorption spectrum of ZnO nanorods prepared at the 95 ^{o}C for 3.5 h for the three preparation ways (no air bubbles, air bubbles and Oxygen bubbles). This spectrum reveals that low concentration ZnO film has a low absorbance in the visible region,

which is a characteristic of ZnO [33]. The absorbance has increased when the air and oxygen bubbles involved in the preparation process and this means that the optical properties have been changed. The maximum of absorption also shifted to longer wavelengths, that about 405 nm, 397 nm and 388 nm for no air bubbles, air bubbles and oxygen bubbles respectively. The optical band gap of ZnO nanorods was determined by the extrapolation of the linear portion of $(\alpha h\nu)^2$ versus hν plots using Tauc formula [34]:

$$(\alpha h\nu)^2 = A(h\nu - E_g)^n \quad (7)$$

Where α is the absorption coefficient, hν is the photon energy, A is constant, E_g is the optical band gap energy and n depends on the transmission type (equals to 1 for allowed direct transmission).

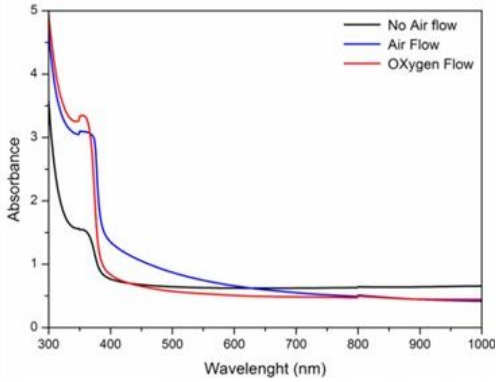

Fig. 6 Optical absorption spectrum of ZnO nanorods at 95 °C for 3.5h for the three different ways

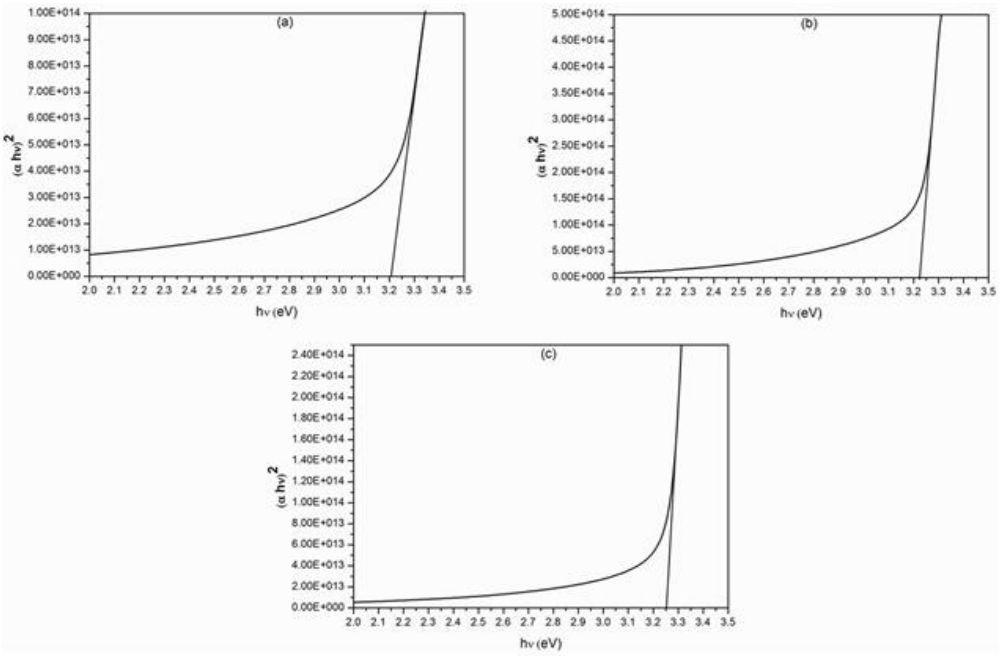

Fig. 7 Band gap energy spectra of ZnO nanorods prepared by modified CBD
(a) No Air Bubbles, (b) Air Bubbles, (c) Oxygen Bubbles

Fig. 7 shows the Tauc plot for the three different ZnO nanorods preparation ways film which they are no air bubbles, air bubbles and oxygen bubbles. The plots are clearly shows that the transition region around 3.2 eV and it correspond to the direct transition band between the edges of

valance and conduction bands which represent the optical energy gap of ZnO semiconductor. Regarding to the plot, it exactly found the band gap energy of ZnO nanorods increase with injection air and oxygen bubbles inside the CBD reactor, i.e. 3.21 eV, 3.24 eV and 3.26 eV for no air bubbles, air bubbles and oxygen bubbles respectively. And obtained results are agreed with literatures for single crystal ZnO [35].

4. Conclusion

In this study, one can concludes that this modification of chemical bath deposition method shows the improved results over conventional chemical bath deposition method. This modified CBD method decreases the growth time rate of ZnO nanorods to about 1.5 h compared with previous studied. It is observed from XRD patterns that the introducing of the air and oxygen bubbles causes a reorientation of a nanostructure of ZnO towards [002] direction. The crystal size of ZnO nanorods are decreased by injection air and oxygen bubbles inside the CBD reactor. From FESEM results one can notice that the ZnO nanorods fabricated by introducing oxygen bubbles are denser, less diameter and less length than ZnO nanorods synthesized by introducing air bubbles. It is found from UV spectrum that the energy band gap is increased when the air and oxygen bubbles are involved in the preparation process and this means that the modified CBD process is also make modification to the optical properties of ZnO nanorods.

References

[1] H. Morkoc, U., Ozgur, General Properties of ZnO, in: Zinc Oxide: Fundamentals, materials and device technology, Wiley-VCH Verlag GmbH & Co. KGaA, 2009, pp. 1-76.
[2] S.S. Shinde, K.Y. Rajpure, Appl. Surf. Sci. **257**, 9595 (2011).
[3] Y. Ryu, T.S. Lee, B.J. Kim, Y.S. Park, C.J. Youn, Appl. Phys. Lett. **88,** 241108-1 (2006).
[4] A.I. Hochbaum, P. Yang, Chem. Rev. **110**, 527 (2010).
[5] L.nHey-Jin, Y. L. Deuk, O. Young, Sensors and Actuators A: Physical, **125**(2), 405 (2006).
[6] R Marte, T Schmidt, H R Shea, et al. Appl. Phys. Lett., , **73**(17), 2447 (1998).
[7] M.H. Huang, S. Mao, H. Feick, H.G. Yan, Y.Y. Wu, H. Kind, E. Weber, R. Russo, P.D. Yang, Science **292,** 1897 (2001).
[8] W.I. Park, D.H. Kim, S.W. Jung, G.C. Yi, Appl. Phys. Lett. **80**, 4232 (2002).
[9] H W Suh, G Y Kim, Y S Jung, W K Choi, D.Byun Journal of Applied Physics, **97**(4), 044305 (2005).
[10] G. Yi, C. Wang, W.I. Park, Semicond. Sci. Technol. **20**, S22 (2005).
[11] S.C. Tjong, Nanocrystalline materials: their Synthesis- Structure Property Relationships and Applications, Elsevier Ltd, 2006.
[12] D. B. Mitzi, Solution processing of inorganic materials, John Wiley & Sons, Inc., Hoboken, New Jersey, 2009.
[13] M.E. Fragala, C. Satriano, G. Malandrino, Chem. Commun. (2009) 839–841.
[14] H.D. Yu, Z.P. Zhang, M.Y. Han, X.T. Hao, F.R. Zhu, J. Am. Chem. Soc. **127,** 2378 (2005).
[15] Y. Sun, G.M. Fuge, M.N.R. Ashfold, Chem. Phys. Lett. **396**, 21 (2004).
[16] A. El Hichou, M. Addou, A. Bougrine, R. Dounia, J. Ebothé, M. Troyon, M. Amrani. Materials Chemistry and Physics. **83**(1):43 (2004).
[17] A. Dadgar, N. Oleynik, D. Forster, S. Deiter, H. Witek, J. Bläsing, F. Bertram, A. Krtschil A. Diez, J. Christen, et al., Crystal Growth, **267(**1-2), 140 (2004).
[18] Z. Guo, D.X. Zhao, Y. Liu, D. Shen, J. Zhang, B. Liu, Appl. Phys. Lett. **93**, 1 (2008).
[19] P. Yang, H. Yan, S. Mao, R. Russo, J. Johnson, R. Saykally, N. Morris, J. Pham, R. He, H.-J. Choi, Adv. Funct. Mater. **12**, 323 (2002).
[20] P.M., Aneesh, K.A Vanaja, M.K., Jayaraj, Proc. SPIE 6639, Nanophotonic Materials IV, 66390J. (September 17, 2007).
[21] M.G. Varnamkhasti, H.R. Fallah, M. Zadsar, Vacuum **86**, 871 (2012).
[22] K.M. McPeak, J.B. Baxter, Ind. Eng. Chem. Res. **48**, 5954 (2009).

[23] J.Y. Jung, N. Park, S. Han, G.B. Han, T.J. Lee, S.O. Ryu, C. Chang, Curr. Appl. Phys. **8**, 720 (2008).
[24] H. Zhang, J. Feng, J. Wang and M. Zhang, Materials Letters **61**, 5202 (2007).
[25] M. Kashif, U. Hashim,1 M. E. Ali, Syed M. Usman Ali, M. Rusop, Z. H. Ibupoto, M. WillanderHindawi Publishing Corporation Journal of Nanomaterials ,V. 2012, Article ID 452407, 6 pages.
[26] C Suryanarayana, G Norton: X-Ray Diffraction: A Practical Approach. Springer Science + Business Media, LLC, 233 Spring Street, New York, NY 10013, USA: Plenum Press; 1998.
[27] B.E. Warren, X-ray Diffraction (Courier Dover Publications, New York, 1969).
[28] H. Lipson, Contemp. Phys. **20**, 87 (1979).
[29] C.-Y. Tsay, K.-S. Fan, S.-H. Chen, C.-H. Tsai, J. Alloys Compd. **495**, 126 (2010).
[30] B.D.Cullity, Elements of X-ray Diffraction, second edition, Addison Wesley (2007).
[31] A.H. Kurda, Y. M. Hassan, N. M. Ahmed, World Journal of Nano Science and Engineering, **5**, 34 (2015).
[32] M. Thambidurai, N. Muthukumarasamy, D. Velauthapillai, C. Lee, Solar Energy **106,** 143 (2014).
[33] R Chandramohan, T A Vijayan, S Arumugam, H B Ramalingam, V Dhanasekaran, K Sundaram, T Mahalingam Mater. Sci. Engg. B **176,** 152 (2011).
[34] J. Tauc, R. Grigorovici, A. Vancu, Phys. Status Solidi B **15**, 627 (1966).
[35] V. Srikant, D. R. Clarke, , J. Appl. Phys. **83**, 5447 (1998); doi: 10.1063/1.367375